COMPUTATIONAL ANALYSIS OF STRUCTURAL STABILITY AND RESISTANCE TO GAMMA AND ELECTRON RADIATION IN LMO AND LNMO SPINELS.

ANÁLISIS COMPUTACIONAL DE LA ESTABILIDAD ESTRUCTURAL Y LA RESISTENCIA A LA RADIACIÓN GAMMA Y ELECTRÓNICA EN ESPINELAS LMO Y LNMO.

D. Valdés†, A. Leyva, C. Cruz

Centro de Aplicaciones Tecnológicas y Desarrollo Nuclear (CEADEN), La Habana, Cuba. valdeslozada99@gmail.com
† corresponding author

Recibido 21/10/2025; Aceptado 26/3/2026

This study investigates the response to gamma and electron radiation of materials used as cathodes in lithium-ion batteries, specifically $LiMn_2O_4$ (LMO) and $LiNi_{0.5}Mn_{1.5}O_4$ (LNMO), through the computational analysis of displacement cross-sections per atom. The results indicate that the partial substitution of Mn with Ni in LNMO significantly increases radiation resistance, which is attributed to the strengthening of Ni-O covalent bonds, the reduction of Jahn-Teller distortions, and the stabilization of the crystal lattice. Monte Carlo simulations using the MCCM software reveal that LNMO requires energies $1.3 - 1.8$ times higher for the initiation of atomic displacement cascades compared to LMO.

Este estudio investiga la respuesta a la radiación ganma y electrónica de materiales empleados como cátodo en baterías de iones de litio, específicamente $LiMn_2O_4$ (LMO) y $LiNi_{0.5}Mn_{1.5}O_4$ (LNMO), mediante el análisis computacional de las secciones eficaces de desplazamientos por átomo. Los resultados indican que la sustitución parcial de Mn por Ni en el LNMO incrementa significativamente la resistencia a la radiación, lo cual se atribuye al fortalecimiento de enlaces covalentes Ni-O, la reducción de las distorsiones Jahn-Teller y la estabilización de la red cristalina. Las simulaciones por Monte Carlo usando el software MCCM revelan que el LNMO requiere de energías $1,3 - 1,8$ veces mayores para que se dé inicio a las cascadas de desplazamiento atómico en comparación con LMO.

Keywords: spinel materials (materiales de espinela), radiation damage (daño por radiación), threshold displacement energy (energía umbral de desplazamiento), lithium-ion batteries (baterías de iones de litio), atomic displacement cascades (cascadas de desplazamiento atómico)

I. INTRODUCTION

Spinel compounds, characterized by the general formula AB_2O_4 and a robust three-dimensional crystal structure (space group $Fd\bar{3}m$) [1], constitute a critically important class of electrode materials for advanced rechargeable battery systems, particularly lithium-ion batteries (LIBs). Their appeal stems from an advantageous combination of structural stability, high operational voltage, and promising rate capability [2]. The archetypal framework consists of a cubic close-packed (ccp) array of oxide anions (O^{2-}), where the A^{2+} cations occupy one-eighth of the tetrahedral sites (Wyckoff position 8a) and the B^{3+} cations reside in half of the octahedral sites (16d) [3] [4]. In electrochemically active lithium-based spinels (e.g., $LiMn_2O_4$), the A site is occupied by Li^+ ions, while the B site is filled by transition metal ions (e.g., Mn^{3+}/Mn^{4+} or Ni^{2+}), whose redox activity enables lithium (de)intercalation.

This arrangement confers unique properties: high ionic conductivity, thermal stability, and resistance to extreme conditions [5]. The substitution of Mn by Ni in $LiMn_2O_4$ (LMO) generates $LiNi_{0.5}Mn_{1.5}O_4$ (LNMO) , altering the cation distribution and modifying electronic interactions, which directly impacts the threshold displacement energy (TDE) [6].

Previously, it has been experimentally demonstrated that gamma radiation significantly modifies the electrochemical properties of spinel cathodes [7], due to the generation of structural defects. However, the atomic origin of these changes — in particular, the atomic displacements induced by secondary electrons — has not been quantified in LMO and LNMO. Therefore, the present work determines, for each atom and according to its crystallographic position (tetrahedral or octahedral), the probability of atomic displacement and the associated threshold energies, thereby providing a mechanistic explanation for the greater stability of LNMO against radiation.

II. II. FUNDAMENTALS

II.1. II.1 Cation distribution and threshold displacement energy (TDE)

The unit cell of the spinel contains 56 atoms [8], with a generalized structural formula:

$$[A_{8a}][B_{16d}]_2O_{32e}$$

The structural stability of these materials under irradiation is a critical aspect; a key parameter for evaluating this stability is the TDE, defined as the minimum energy required to displace an atom from its position in the crystal lattice and create a

primary defect, such as a Frenkel pair. The TDE depends on multiple factors, including the crystal structure, the nature of chemical bonds, atomic mass, and crystallographic direction [9].

For the spinel structure of LMO, the cation distribution can be expressed as:

$$L_{spinel} = (Li^{+})_{8a}[Mn^{3+/4+}]_{16d}(O^{2-})_{32e} \quad (1)$$

In LNMO:

$$L_{LNMO} = (Li^{+})_{8a}[Ni^{2+/3+}_{16d}, Mn^{3+/4+}_{16d}](O^{2-})_{32e} \quad (2)$$

The TDE is related to crystal stability under radiation through models such as Kinchin–Pease and NRT (Norgett–Robinson–Torrens) [10]:

$$N_{d,\mathrm{NRT}}(T_d) = \begin{cases} 0 & T_d < E_d \\ 1 & E_d < T_d < 2E_d \\ \eta \dfrac{T_d}{2E_d} & T_d > 2E_d \end{cases}, \quad (3)$$

where N_d is the number of displacements per atom, T_d is the deposited energy, E_d is the TDE, and η is the damage efficiency (~ 0.8) [11].

In the spinel structure, atoms in octahedral sites, such as Mn in LMO, generally exhibit a higher TDE than atoms in tetrahedral sites, such as Li, due to a greater number of bonds and higher local atomic density [12]. Covalent bonds, such as Ni–O in LNMO, are stronger than predominantly ionic bonds, such as Li–O in LMO, which also contributes to a higher TDE [13]. Furthermore, lighter atoms, such as Li, require less energy to be displaced than heavier atoms such as Mn or Ni [14]. It has been suggested that the presence of Jahn-Teller distortions, characteristic of Mn^{3+} in LMO, could weaken the lattice and contribute to a reduction in the TDE [15].

II.2. II.2 Effects of Ni doping

The substitution of Mn^{3+} by Ni^{2+}/Ni^{3+} in LMO not only oxidizes part of the Mn to Mn^{4+}, but also appears to significantly reduce Jahn-Teller distortions, which potentially stabilizes the crystal structure and strengthens the Ni–O and Mn^{4+}–O bonds [16]. The substitution of Mn by Ni increases the effective local atomic density due to the higher atomic mass of nickel (58.7 vs. 54.9 u). This increased density contributes to a greater number of effective nearest neighbors and strengthens the local network, thereby raising the energy barriers for atomic displacement. The TDE of Ni atoms in LNMO is estimated to be between 70–120 eV, reflecting the strength of its covalent bonds with oxygen. These increases in TDE are directly proportional to the concentration of Ni, making LNMO more resistant to irradiation damage than LMO.

II.3. II.3 Atomic displacement cascades

When a target atom (the lattice atom) receives a recoil kinetic energy from an incident particle, becoming a Primary Knock-on Atom (PKA), that exceeds its TDE, a displacement is initiated. This results in the atom being ejected from its lattice site. This displaced atom can collide with other neighboring atoms, transferring the remaining energy (in terms of kinetic energy) to other atoms. If this energy is sufficiently high, it can provoke an atomic displacement cascade that propagates through the crystal lattice, thus generating a large number of point defects such as vacancies and interstitials [17]. In the case of gamma irradiation, the maximum kinetic energy that a secondary electron can acquire is equal to the energy of the incident photon itself. The average energy transferred from such an electron to a PKA can be estimated by:

$$T = \frac{2E_e^2}{m_e c^2 + 2E_e}, \quad (4)$$

where E_e is the energy of the electron, m_e the rest mass of the electron and c the speed of light in vacuum. For relativistic approximations, though in practice for gamma interactions, compton scattering dominates and the maximum electron recoil energy determines the potential for secondary ionization and, indirectly, atomic displacements. The gamma radiation considered in this work comes from a ^{60}Co source (1.17 and 1.33 MeV), consistent with the source available in our laboratory. These photon energies exceed typical TDE values, generating secondary electrons (Compton and photoelectric) that induce PKAs. The kinetic energy of these secondary electrons is used as input for the displacement cascade simulations.

III. III. MATERIALS AND METHODS

Given that the TDE for atoms within LMO and LNMO spinels have not been experimentally established, TDE values were inferred from those of atoms occupying similar lattice sites in compounds with analogous chemical bonding and crystal symmetry. In particular, experimental and computational studies on structurally related spinel oxides such as $MgAl_2O_4$, $LiFe_5O_8$, and $NiCr_2O_4$ were analyzed to infer trends in bond strength, coordination, and radiation response [18] [19] [20]. Based on this comparative research, an approximation for the TDE values in LMO (Table I) and LNMO (Table II) was proposed, guided by systematic trends in atomic mass, cation–oxygen bond covalency, and geometry site(tetrahedral vs. octahedral). First-principles calculations on analogous systems support that TDE ranges with local atomic density and bond strength, allowing reasonable extrapolation to LMO and LNMO [18] [19] [20].

Table 1. Ranges of displacement threshold energy for $LiMn_2O_4$

Atom	Z	$E_d^{\min}$(eV)	$E_d^{\max}$(eV)	E_d^{prom}(eV)
Li	3	10	100	20
Mn	25	40	100	70
O	8	40	70	55

Table 2. Ranges of displacement threshold energy for $LiNi_{0.5}Mn_{1.5}O_4$

Atom	Z	$E_d^{\min}$(eV)	$E_d^{\max}$(eV)	E_d^{prom}(eV)
Li	3	25	50	37.5
Ni	28	70	120	95
Mn	25	90	130	110
O	8	50	100	75

The phenomenon of atomic displacement cascades can be analyzed through the calculation of displacements per atom (dpa) cross-section, which quantifies the probability of total accumulated damage in the lattice. The cutoff energy values for the initiation of simple atomic displacement processes (E_c), related to the TDE, can be calculated using the equation;

$$E_c = \frac{2E_d}{1-\alpha}, \tag{5}$$

where α is a factor depending on the mass of the involved atoms.

For the calculation of the dpa cross-section and E_c, the Monte Carlo assisted Classical Method (MCCM) program [21] was used, which employs classical theories of electron elastic scattering. The MCCM program uses only elastic electron scattering because elastic nuclear collisions transfer significant energy to atoms, while inelastic processes (ionization, etc.) produce secondary electrons with energies below the displacement threshold. Thus, inelastic contributions to atomic displacement are negligible, a standard approximation in computational radiation damage studies. The cutoff energies for the initiation of atomic displacement cascades (E_{cc}) were obtained by plotting the results from MCCM (dpa cross-section vs. kinetic energy) and determining the point at which the slope of the curve changes.

IV. IV. RESULTS AND DISCUSSION

Figures 1, 2, and 3 illustrate the calculation of dpa cross-section using the minimum, maximum, and average values of the TDE for each atom in LMO. The calculation of dpa cross-section using the minimum, maximum, and average values of the TDE for each atom in LNMO are shown in figures 4, 5 and 6.

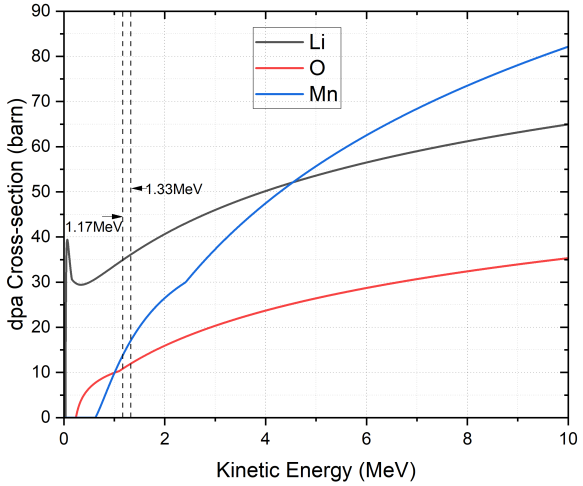

Figure 1. Relationship of dpa cross-section versus kinetic energy for the minimum TDE values of LMO.

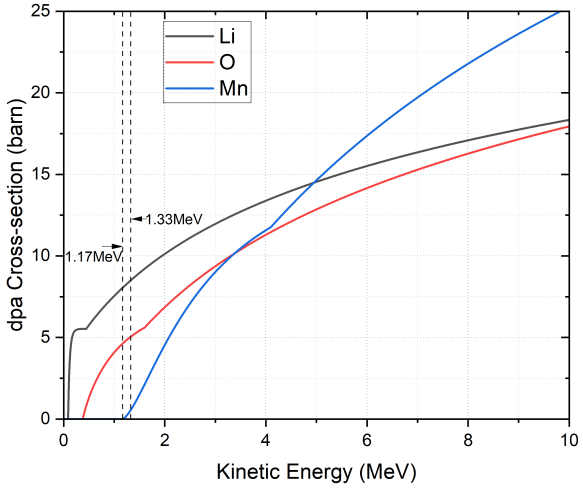

Figure 2. Relationship of dpa cross-section versus kinetic energy for the maximum TDE values of LMO.

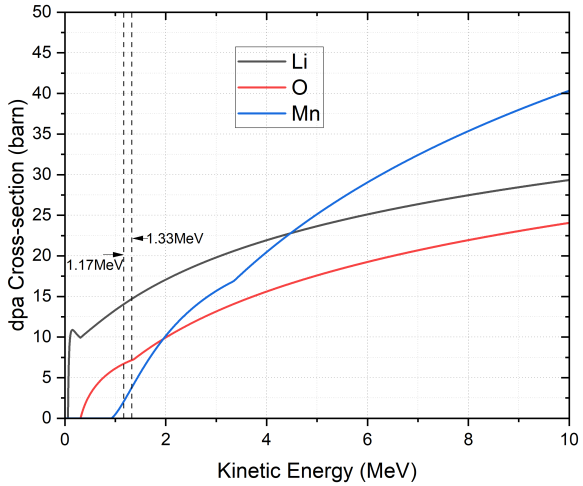

Figure 3. Relationship of dpa cross-section versus kinetic energy for the average TDE values of LMO.

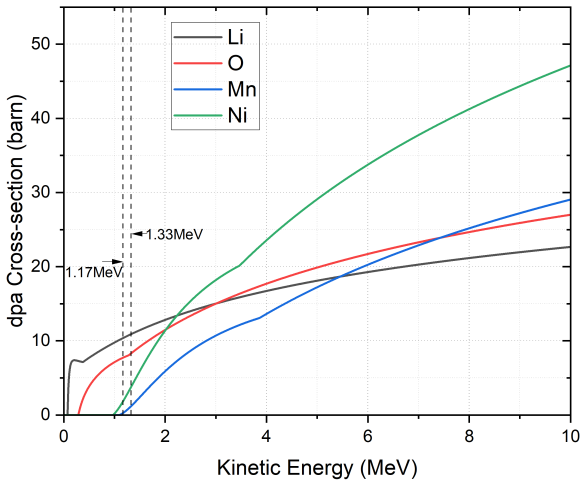

Figure 4. Relationship of dpa cross-section versus kinetic energy for the minimum TDE values of LNMO.

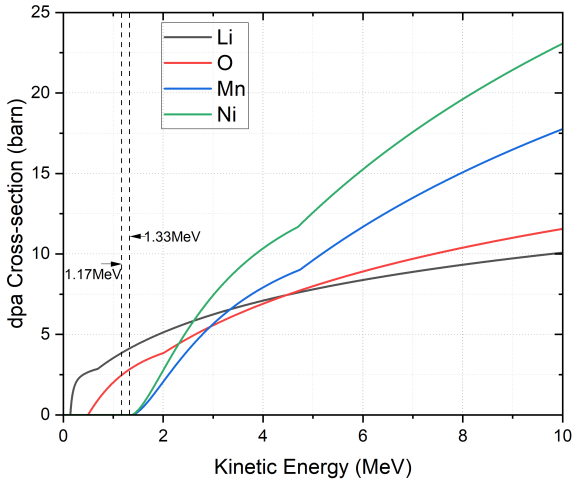

Figure 5. Relationship of dpa cross-section versus kinetic energy for the maximum TDE values of LNMO.

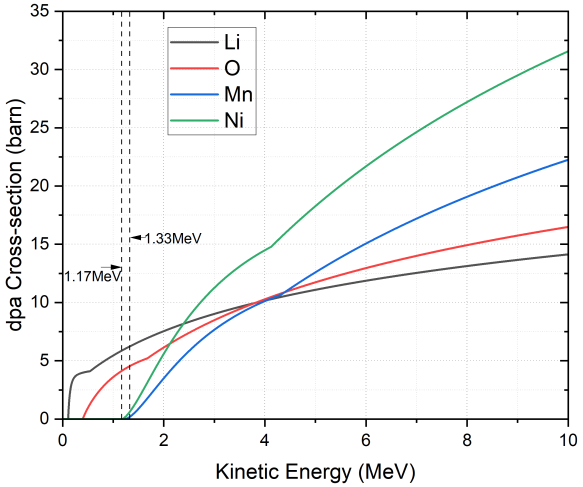

Figure 6. Relationship of dpa cross-section versus kinetic energy for the average TDE values of LNMO.

From the graphs, E_c and E_{cc} were extracted for each TDE value of atom in LMO (Table III) and LNMO (Table IV).

Table 3. Cutoff energy values for the initiation of simple atomic displacement processes and cutoff energies for the initiation of atomic displacement cascades, corresponding to each TDE value of each atom in LMO.

Atom	Z	E_d (eV)	E_c (MeV)	E_{ci} (MeV)
Li	3	10	0.031	0.157
		30	0.088	0.448
		20	0.060	0.308
Mn	25	40	0.626	2.411
		100	1.174	4.098
		70	0.926	3.347
O	8	40	0.238	1.096
		70	0.376	1.604
		55	0.310	1.365

Compared to Li, the Mn and Ni bonds require 2 to 3.6 times more displacement energy, reflecting their stabilizing role in the lattice. The probability of initiating a cascade is directly determined by the TDE; therefore, materials with high TDE, such as LNMO, have a higher threshold for cascade initiation, reducing the probability of forming cascades and thereby minimizing accumulated structural damage. Monte Carlo simulations reveal that the dpa cross-sections for LNMO are systematically lower than those for LMO under equivalent irradiation conditions. This reduction is directly attributed to the higher TDE, which require greater energy to initiate damage processes. The relationship between TDE and damage accumulation follows trends predicted by theoretical models: materials with higher TDE accumulate fewer defects per unit of radiation dose, resulting in better stability of structural and electrochemical properties under prolonged irradiation.

Table 4. Cutoff energy values for the initiation of simple atomic displacement processes and cutoff energies for the initiation of atomic displacement cascades, corresponding to each TDE value of each atom in LNMO.

Atom	Z	E_d (eV)	E_c (MeV)	E_{ci} (MeV)
Li	3	10	0.031	0.157
		30	0.088	0.448
		20	0.060	0.308
Mn	25	40	0.626	2.411
		100	1.174	4.098
		70	0.926	3.347
O	8	40	0.238	1.096
		70	0.376	1.604
		55	0.310	1.365

V. CONCLUSIONS

This study indicates that the substitution of Mn by Ni in LNMO not only improves its electrochemical properties but also significantly increases its resistance to irradiation damage. Strengthening of Ni-O covalent bonds and oxidation of Mn^{3+} to Mn^{4+} may reduce Jahn-Teller distortions, which in turn could contribute to an elevation of the threshold displacement energy of the constituent atoms. The increase in TDE translates into a higher critical energy (E_c) and cascade initiation energy (E_{cc}), which decreases the probability of forming point defects and atomic cascades. The calculation of the dpa cross-section confirms that LNMO accumulates less structural damage for the same irradiation dose.

REFERENCES

[1] G. B. Andreozzi and F. Princivalle, Am. Mineral. **87**, 838 (2002).
[2] Y. Lin, F. Li, K. Zhao, S. Zou, X. Tan, Z. Shi, J. Fan, L. Ouyang, M. Zhu, and J. Liu, Small Methods **9**, 2402233 (2025).
[3] H. Sun et al., Adv. Funct. Mater. **32**, 2112279 (2022).
[4] L. Wan, Y. Deng, C. Yang, H. Xu, X. Qin, and G. Chen, RSC Adv. **12**, 30503 (2022).
[5] M. M. Thackeray, P. J. Johnson, J. T. Vaughey, N. Li, and S. A. Hackney, J. Mater. Chem. **15**, 2257 (2005).
[6] K. E. Sickafus et al., Science **289**, 748 (2000).
[7] R. Arabolla et al., Solid State Ionics **324** (2018).
[8] C. Biagioni and M. Pasero, Am. Mineral. **99**, 1254 (2014).
[9] P. Dzerzanovsky and I. G. Barash, Geol. Ore Deposits **53**, 758 (2011).
[10] I. M. Torrens and M. T. Robinson, Phys. Rev. B **9**, 5008 (1974).
[11] M. J. Norgett, M. T. Robinson, and I. M. Torrens, Nucl. Eng. Des. **33**, 50 (1975).

[12] R. Amin and I. Belharouk, J. Power Sources **348**, 311 (2017).
[13] M. Kunduraci, J. F. Al-Sharab, and G. G. Amatucci, Chem. Mater. **18**, 3585 (2006).
[14] J. H. Kim, N. P. W. Pieczonka, Z. Li, Y. Wu, S. Harris, and B. R. Powell, Electrochim. Acta **90**, 556 (2013).
[15] L. Cai, Z. Liu, K. An, and C. Liang, J. Mater. Chem. A **1**, 6908 (2013).
[16] A. J. A. Al-Hail et al., ACS Appl. Energy Mater. **3**, 6400 (2020).
[17] M. T. Robinson and I. M. Torrens, Phys. Rev. B **9**, 5008 (1974).
[18] W. A. Coghlan, F. W. Clinard, N. Itoh, and L. R. Greenwood, J. Nucl. Mater. **141–143**, 382 (1986).
[19] S. Tan, W. Zhang, F. Jiao, Y. Zhou, L. Yang, W. Shi, and Z. Wang, Cryst. Res. Technol. **56**, 2100076 (2021).
[20] L. Van Brutzel, P. Alvarez, and A. Chartier, Nucl. Instrum. Methods Phys. Res. B **326**, 278 (2014).
[21] I. Piñera, C. M. Cruz, Y. Abreu, A. Leyva, A. E. Cabal, and P. Van Espen, in 2008 IEEE Nuclear Science Symposium Conference Record, 2557 (2008).